Protein-Mediated Assembly of Nanodiamond Hydrogels into a Biocompatible and Biofunctional Multilayer Nanofilm

Houjin Huang,[†] Erik Pierstorff,[†] Eiji Osawa,[‡] and Dean Ho[†,§,*]

[†]Departments of Biomedical and Mechanical Engineering, Robert R. McCormick School of Engineering and Applied Science, Northwestern University, Evanston, Illinois 60208, [‡]NanoCarbon Research Institute, Ltd., Asama Research Extension Center, Shinshu University, 3-15-1 Tokita, Ueda, Nagano 386-8567, Japan, and [§]Robert H. Lurie Comprehensive Cancer Center, Feinberg School of Medicine, Northwestern University, Chicago, Illinois 60611

ABSTRACT Aqueous dispersible detonation nanodiamonds (NDs) with a diameter of 2–8 nm were assembled into a closely packed ND multilayer nanofilm with positively charged poly-L-lysine *via* the layer-by-layer deposition technique. The innate biocompatibility of the NDs in both free-floating and thin-film forms was confirmed *via* cellular gene expression examination by real-time polymerase chain reaction as well as MTT and DNA fragmentation assays. The highly biologically amenable ND nanofilm was successfully integrated with therapeutic molecules, and the functionality of the composite drug—ND material was assessed *via* interrogation of the suppression of inflammatory cytokine release. Knockdown of lipopolysaccharide-mediated inflammation was observed through the potent attenuation of tumor necrosis factor-alpha, interleukin-6, and inducible nitric oxide synthase levels following ND nanofilm interfacing with RAW 264.7 murine macrophages. Furthermore, basal cytokine secretion levels were assessed to examine innate material biocompability, revealing unchanged cellular inflammatory responses which strongly supported the relevance of the NDs as effective treatment platforms for nanoscale medicine. In addition to the easy preparation, robustness, and fine controllability of the film structures, these hybrid materials possess enormous potential for biomedical applications such as localized drug delivery and anti-inflammatory implant coatings and devices, as demonstrated *in vitro* in this work.

KEYWORDS: nanomedicine · nanodiamond · bionanotechnology · drug delivery · biointerface · coating

In recent years, nanobiotechnology, as a branch of nanotechnology with an emphasis on biological perspectives, has attracted much attention.[1] This technology involves studies of natural or artificial nanostructures for biological applications and the fabrication of biofunctional devices from the integration of these nanostructures.[2,3] Among the various nanoscale elements that are currently being explored for biological applications, carbon-based nanomaterials [*e.g.*, fullerene, carbon nanotubes (CNTs), and nanodiamonds (NDs)] are receiving much attention due to their remarkable physical, chemical, and biological properties.[4–6] With respect to the application of nanocarbon materials in a biological or medical context, the scientific community has thus far been primarily focused on fullerene- and CNT-based modalities, while their biocompatibility in the form of material-induced cyto-regulatory activity still receives continued evaluation.[7,8]

Owing to their superior chemical and physical properties as well as biocompatibility, diamond-based nanostructures have emerged as promising alternative materials for biomedical applications. Previous work has examined the use of ultrananocrystalline diamond thin films produced by chemical vapor deposition (CVD) for robust implant coatings and biosensors,[9,10] as well as fluorescent ND particles (35 and 100 nm diameters) for biological tagging and imaging applications.[11,12] Recently, NDs with a much smaller size (<10 nm diameter) generated by the detonation technique have attracted much attention due to their advantageous dimensional properties that enable favorable interfacing with biological systems.[13–17] The dispersion of detonation NDs in aqueous media made by Osawa and colleagues has facilitated the use of NDs in physiological systems.[14] The biocompatibility of detonation NDs from the standpoint of cell viability and proliferative behavior has also been recently assessed. Mitochondrial function (MTT) and luminescent ATP production assays showed that the NDs are not toxic to a variety of cell types.[15] Compared to other nanocarbon materials such as CNTs, which have been shown to be toxic in many studies and are naturally not water-soluble, it is thus

*Address correspondence to d-ho@northwestern.edu.

Received for review July 5, 2007 and accepted January 17, 2008.

Published online February 1, 2008.
10.1021/nn7000867 CCC: $40.75

envisaged that NDs can serve as an enhanced/versatile material for biomedical applications in physiological systems.[12,16]

Current techniques of producing ultrananocrystalline diamond thin films *via* CVD processing involve a gas-phase chemical reaction occurring above limited types of solid surfaces, which also requires costly instrumentation (reactors, vacuum furnaces, heaters, plasma generators, *etc.*) and extreme reaction conditions, such as precisely controlled gas flow, high vacuum parameters, and high temperatures (>1000 K).[9] For biomedical applications, a more critical concern pertains to the notion of whether the generated diamond film, which is typically very hard, is compatible with soft tissues in the living body and if the material−biology interface induces an inflammatory effect. Therefore, the development of an alternative approach utilizing mild coating conditions, a low-cost fabrication methodology, and the engineering of biofunctionality into the composite nanofilm system is of significant importance.

Alternatively, diamond thin films can also be assembled from a fluorine-functionalized detonation ND powder. Halas and colleagues have recently demonstrated a novel method for generating an ND coating on a glass surface through the reaction of a fluorinated ND powder with an amino-functionalized glass surface.[18] While this coating process is performed at a relatively low temperature (130 °C), the NDs first have to pass through a tedious (48 h), high-temperature (350 °C), and toxic (with F_2 gas) functionalization procedure.[18,19] The reactive coating process then involves the application of a toxic solvent (dichlorobenzene) and can also be time-consuming. Moreover, multilayer coating and drug incorporation into the single-layer film by this method is difficult because of the hydrophobic nature of fluorinated NDs and the covalent linkage that occurs only between the functionalized substrate and the functionalized NDs. In addition, biocompatibility of the fluorine-functionalized NDs has not yet been demonstrated.

In this work, we have developed single-layer and multilayer diamond films assembled from dispersible nontoxic NDs with controllable thickness *via* a soft coating layer-by-layer (LBL) deposition technique (Figures 1 and 2). The LBL method introduced by Decher and coworkers in the early 1990s has attracted extensive attention.[20,21] The extraordinary advantages of this technique for biomedical applications include ease of preparation, versatility with respect to substrate size and topology, capability of incorporating a high loading capacity of different types of biomolecules in the films, fine control over the material structure, and robustness of the products under ambient and physiological conditions.[22] In this work, we also examined the biocompatibility of the NDs in both free-floating and LBL thin-film forms at the gene expression level *via* real-time polymerase chain reaction (RT-PCR), in which

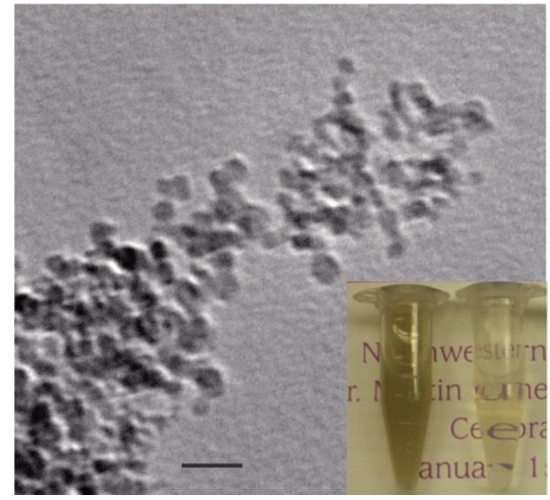

Figure 1. TEM image of media-assisted ball-milled nanodiamonds. The scale bar is 20 nm. The inset shows 1 mg/mL and 0.1 mg/mL ND aqueous suspensions.

pro-inflammatory cytokine levels were examined. This component of the study served as an important interrogation of the ND biointerfacial phenomena generated by inherent material properties, with the results indicating its potential for medical or clinical applicability. Biofunctionality of the LBL ND film as an anti-inflammation drug matrix was also demonstrated *via* observed knockdown of a wide spectrum of cytokines and signaling molecules.

RESULTS AND DISCUSSION

Figure 3 represents characterization data of the NDs used for self-assembly into the nanofilm, which is necessary for illustrating the chemical nature and purity of the materials used in this work. Figure 3a represents the thermogravimetric analysis (TGA) of the NDs. The temperature at maximum weight-loss rate of the NDs was determined to be ~570 °C, and the majority of the NDs (>95%) were oxidized between 495 and 605 °C. Since amor-

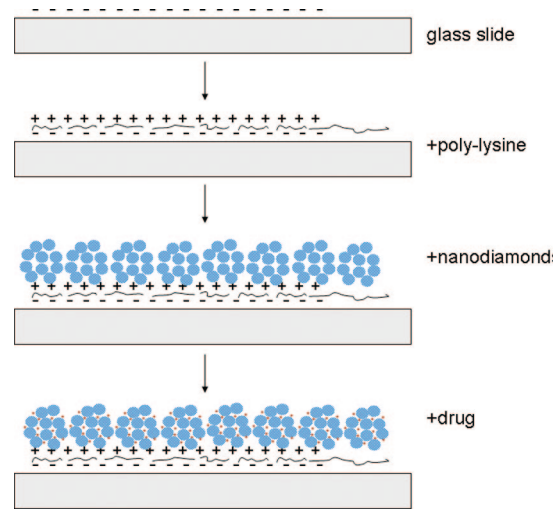

Figure 2. Schematic drawing of nanodiamond nanofilm formation and drug incorporation into the film. Poly-L-lysine is used to attract NDs onto the glass surface.

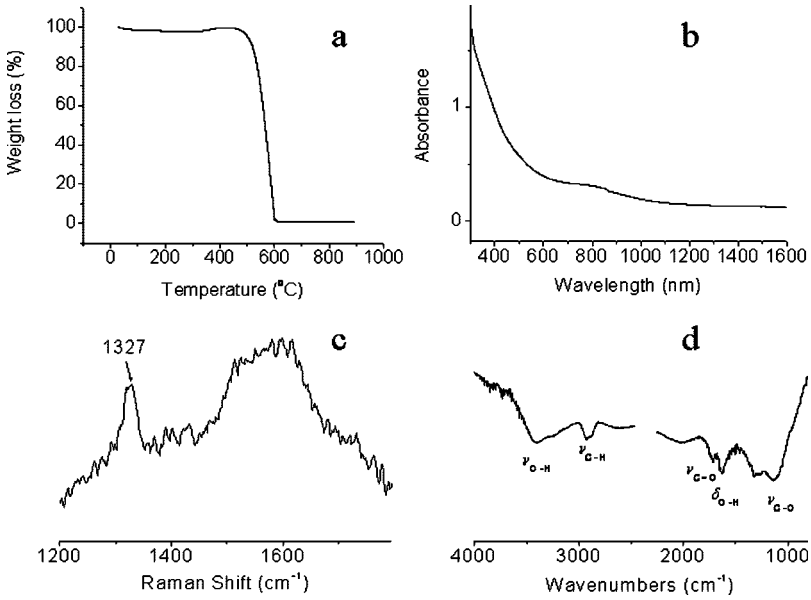

Figure 3. Various characterization modalities employed to examine the nanodiamonds used for self-assembly. (a) Thermogravimetric analysis in air. (b) UV–vis of ND solid deposited on a quartz substrate. (c) Raman scattering. The excitation wavelength of the laser is 514.5nm. (d) FTIR. For FTIR measurements, adsorbed water in NDs was removed by heating the sample in air at 150 °C for 1 h.

phous carbons (<400 °C) and C_{60} (425 °C) are oxidized at much lower temperatures,[23,24] the TGA data shown here clearly indicated that the NDs contained no amorphous carbons and C_{60}. It is also worthy of mention that, due to the size effect, the temperature at maximum weight-loss rate (570 °C) of the NDs was ~60 °C lower than the temperature observed with micrometer-sized diamonds.[24] Another feature in the TGA curve is that the oxidation-induced weight gain around 450 °C, which is due to ND surface fullerene-like conjugated sp^2 carbons, was about 2.2% by weight, indicating that sp^2 carbons comprised 1.7% by atom in terms of one carbon atom reacting with one oxygen atom.

The existence of sp^2 carbons was confirmed by UV–vis, Raman, and FTIR spectroscopy, as shown in Figure 3b–d. Since diamond is a wide bandgap (5.45 eV) semiconductor, pure diamond should not have any optical absorption beyond 300 nm (4.13 eV). But this is not the case for the NDs, as shown in Figure 3b, in which the optical absorption extends toward the near-IR region. This can be attributed to conjugated sp^2 carbons present on ND surfaces. Shown in Figure 3c is the Raman spectra of the NDs. The peak around 1327 cm^{-1} represents clear evidence of the presence of a diamond phase in the sample.[25] As noted by Osawa and colleagues, detonation NDs have never been isolated in pure form.[14] Similar to the formation of fullerols,[26] the fullerene-like surface of NDs,[27] as evidenced by the dark-brown color of the as-received NDs, can be oxidized by strong acid during the purification process, producing many surface-bound –OH and –COOH functional groups, as found in the FTIR spectrum shown in Figure 3d. The rich presence of the functional groups conferred to the NDs two functions, with one being their dispersibility in water and the other being negatively charged surfaces, thus enabling their efficient and ordered self-assembly onto a substrate.

Dispersed NDs can be readily adsorbed onto a poly-L-lysine (PLL)-coated glass slide by dipping the slide into

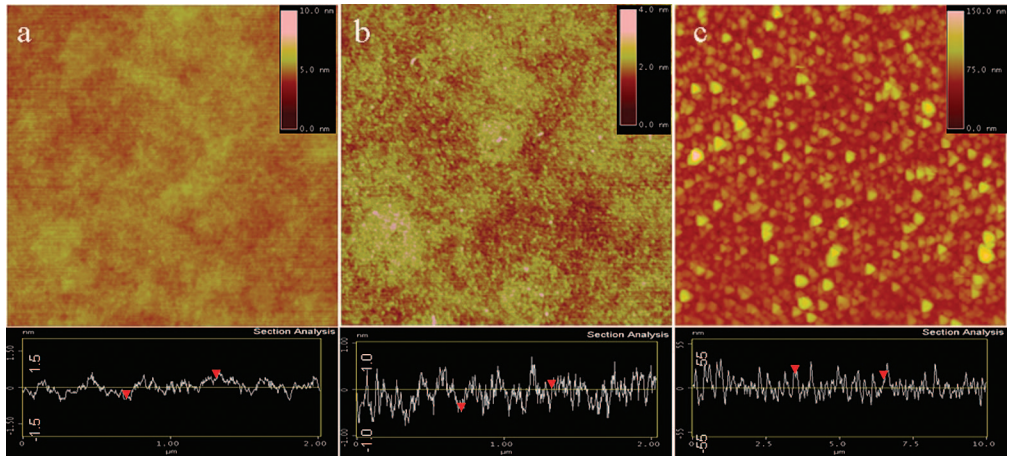

Figure 4. AFM images of (a) bare glass, (b) poly-L-lysine coated on glass, and (c) nanodiamond thin film (one layer) coated on glass. Panels a–c are in height mode, and their sectional analyses are also shown. The scan ranges are 2 μm for all the images.

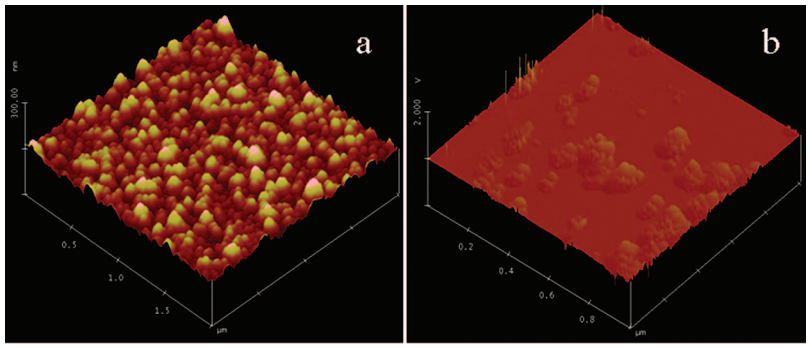

Figure 5. 3-D AFM image of nanodiamond thin film self-assembled from aqueous suspensions (a). For comparison, the morphology of NDs assembled from DMSO suspension is shown in (b).

the ND aqueous solution. Shown in Figure 4a−c are AFM images of bare glass, a PLL-coated slide, and an ND-coated slide, respectively. Tightly packed PLL molecules and ND clusters can be clearly seen. Cross-section analysis indicates that the surface roughness increases from ~0.5 nm for bare glass to ~1.0 nm for a PLL-coated slide and further to ~45 nm for the ND-coated surface. It could clearly be observed that, due to the uniform distribution of the NDs *via* the aforementioned processing methodologies including nitric acid surface treatment, centrifugal purification, milling, and sonication, coupled with PLL-mediated templating, the ND particles were uniformly distributed on the glass slide and no large ND aggregates (>200 m) were observed, resulting from the well-dispersed NDs in water. While other solvents such as dimethyl sulfoxide (DMSO) generate a much higher dispersibility for NDs than water, the NDs were not prone to adsorb on PLL-coated glass under these conditions, as shown in Figure 5b.[17] This may have been due to the aprotic nature of the solvent as well as the affected charge states of the surfaces of the slide as well as the ND particles.

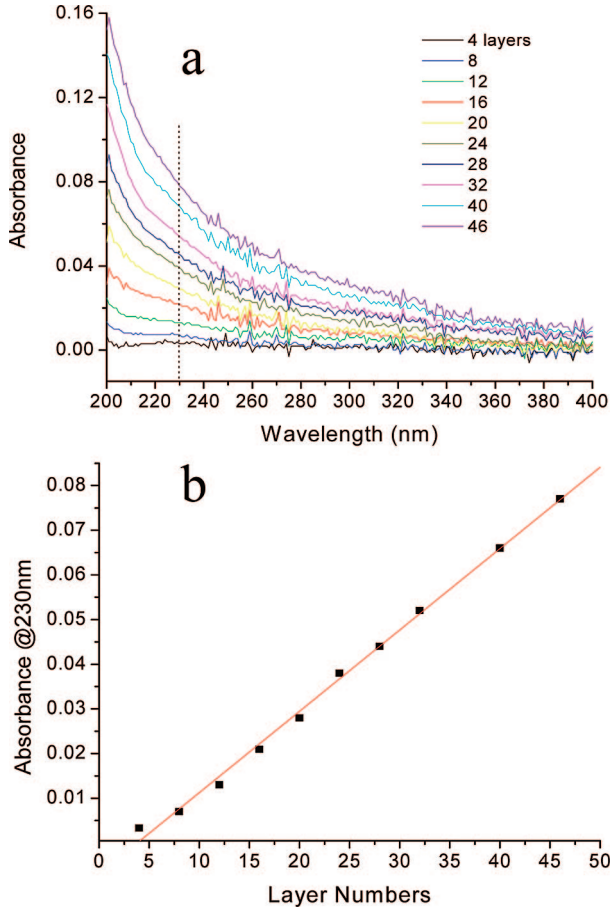

Figure 6. (a) UV–vis spectra of layer-by-layer assembled nanodiamond thin films on quartz substrate. The number of layers is indicated. (b) Optical absorbance of the nanodiamond films measured at 230 nm. The solid line is the linear fitting result.

Taking advantage of UV–vis optical absorption of conjugated sp^2 carbons in NDs, we were able to monitor the construction of ND−PLL multilayers by the LBL technique, as shown in Figure 6. The optical absorbance increased linearly with the subsequent deposition of additional layers. Colorful reflected interference patterns could be seen under light when the number of the layers reached about 10, and disappeared after approximately 20 layers were deposited. From AFM imaging, the surface roughness and morphology of a multilayer ND film of up to 50 layers were essentially the same as those found in a single-layer film. The NDs in the LBL film could not be washed away by vigorous water flow, and thus we believe the film was stably attached onto the glass substrate *via* electrostatic and van der Waals interactions. No film detachment was observed in the salt-containing solutions, which was confirmed by comparing the AFM images before and after cell culture. The ability to construct multilayer structures is particularly important for drug delivery in a medical context because the tuned release of a biological compound (*e.g.*, therapeutic molecules/proteins) can be achieved for basic cellular interfacing studies whereby the LBL method can be used to controllably create multilayers of drug−ND hybrids. In a translational context, novel medical implant coatings can be developed for layer-dependent dosing as well as controllable dosing-rate applications.

To determine the biocompatibility of the constructed ND thin film for potential biomedical applications, cellular effects in response to incubation with free-floating NDs in culture were first investigated. Cell growth and morphology as well as the response of genes involved in inflammation were monitored. Specifically, interleukin-6 (IL-6), tumor necrosis factor alpha (TNFα), and inducible nitric oxide synthetase (iNOS) expression were evaluated using RT-PCR. Shown in Figure 7 (top) is the genetic analysis of inflammation of RAW 264.7 murine macrophages grown for 24 h without and with addition of free-floating NDs (30 μg/mL). No significant change of relative mRNA levels was found for all three genes (TNFα, IL-6, and iNOS) we stud-

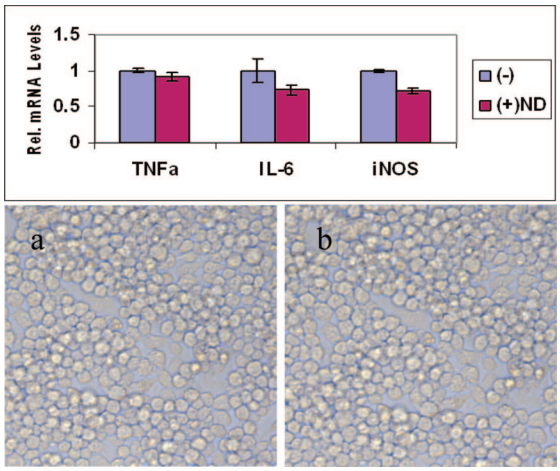

Figure 7. (Top) Genetic analysis (from RT-PCR) of ND innate biocompatibility, performed to monitor inflammation of RAW 264.7 murine macrophage grown for 24 h without and with addition of free-floating nanodiamonds (30 μg/mL). (Bottom) Comparison of the cell morphology grown on glass slides without (a) and with (b) addition of nanodiamond solutions, further confirming the amenability of ND as a suitable bio-interfacial material. The same cell population is utilized to provide an accurate image of the amenability of the nanodiamonds when interfaces with the macrophage cultures.

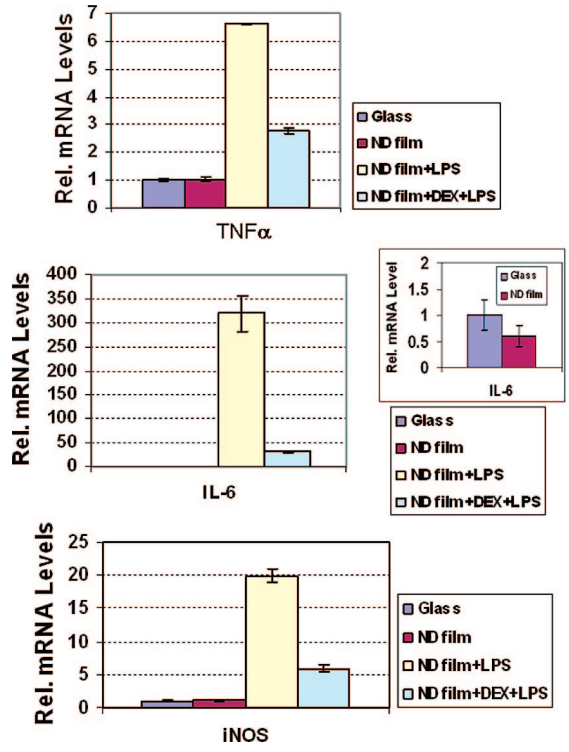

Figure 8. Genetic analysis (from RT-PCR) was performed to monitor the inflammation of RAW 264.7 murine macrophage grown for 24 h on ND films, ND films with lipopolysaccharide (LPS)-mediated inflammation (4 h), and ND−dexamethasone (Dex) films with LPS-mediated imflammation (24 h). Glass slides coated with PLL were used as a control. From top to bottom are gene expression profiles for the inflammatory cytokines TNFα, IL-6, and iNOS, respectively. Results indicate a potent attenuation of LPS-mediated inflammation processes *via* efficient ND−Dex-based blockage of cytokine production. (Inset) The observation that basal IL-6 levels remain unchanged when comparing cells cultured atop glass substrates and ND film–substrates is shown here, given the low levels of IL-6 observed.

ied. In addition, cells were introduced to ND-only solutions, and morphological/architectural characteristics of the cells were monitored. ND solutions were used to introduce a pervasive presence of the NDs toward the cells, which was envisioned to be a more aggressive test of biocompatibility. Both cells with and without the addition of ND solutions grew healthily, with no noticeable cell morphology difference [Figure 7a,b (bottom)]. The same cell population was utilized for Figure 7a,b to demonstrate the lack of adverse effects generated by ND solutions. Additionally, subsequent RT-PCR analysis of cells cultured atop ND films also showed that, at an intrinsic genetic level, the cells were unaffected by the ND substrates, as shown by the absence of ND substrate-mediated up-regulation of inflammatory gene expression (Figure 8). The results are consistent with our previous cell viability studies conducted by examining mitochondrial function (MTT) and luminescent ATP production, indicating that the NDs are significant biocompatible nanomaterials and thus are suitable for implant coatings or as the foundational material for drug delivery devices. We have also examined cell viability and cytokine expression up to a concentration of 100 μg/mL. No apparent cell death in the form of cellular delamination from the ND substrate and inflammation in the form of up-regulated cytokine gene expression, nor cytoxicity and apoptotic induction were observed. The reason we chose 30 μg/mL in addition to 100 μg/mL was to ensure that the NDs did not aggregate during cell growth in culture media. If the concentration were too low, the biocompatibility of NDs may not have been thoroughly properly addressed. As such, because the specified concentration enabled complete film formation while resisting aggregation and served as a favorable fabrication parameter, it was also selected as a concentration for biocompatibility studies.

Genetic analysis was also performed to monitor inflammation of RAW 264.7 murine macrophages grown on ND nanofilms, as shown in Figure 8. Again we confirmed that the ND nanofilm is also biocompatible genetically. Furthermore, ND biocompatibility was analyzed from the standpoint of cytotoxicity in the form of the MTT assay. DNA fragmentation was also used to examine any presence of apoptotic induction due to cellular−ND interactions. RT-PCR studies showed that ND−cellular incubation resulted in maintained levels of IL-6, TNFα, and iNOS when comparing glass-only and ND-only samples (IL-6 comparison shown in Figure 8, inset). This served as one of the many indicators of ND favorability in a biological environment.

Confirmation of dexamethasone (Dex) desorption from the PLL−ND hybrid substrates was examined to confirm that the anti-inflammatory molecules were capable of being eluted from the substrate surface for subsequent activity upon the macrophages. Dex re-

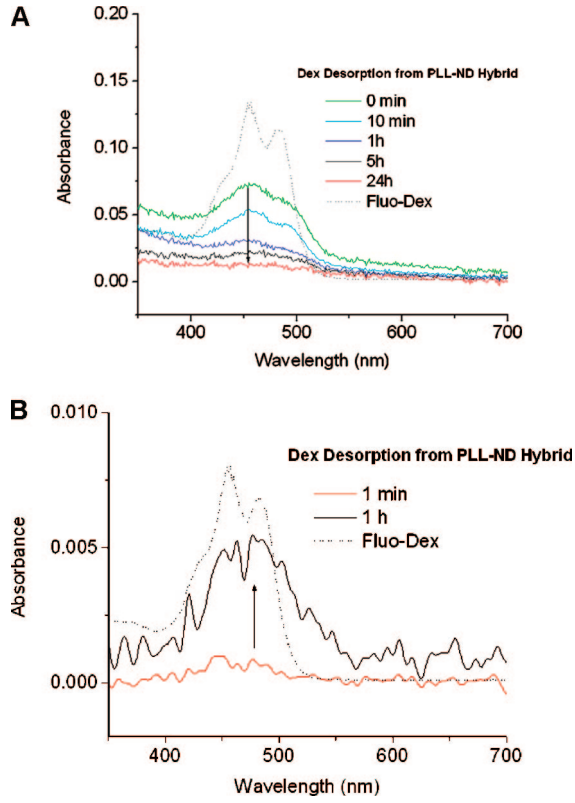

Figure 9. (A) UV–vis spectra of poly-lysine/ND@Dex LBL film (20 layers) on glass, showing that the film continuously releases dexamethasone in water. The dashed line shows the UV–vis spectrum of fluorescent dexamethasone. This confirms that the Dex is capable of being eluted in a sustained fashion from the PLL-supported ND film. (B) UV–vis spectra of fluorescent dexamethasone released from the poly-lysine/ND@Dex LBL film in water using a single-layer hybrid film. The dashed line shows the UV–vis spectrum of fluorescent dexamethasone.

lease was characterized using two substrate conditions, with one being based upon a single PLL−ND hybrid layer, and the other being based upon 20 layers of the PLL−ND surfaces to illustrate in a more pronounced fashion the detachment/delivery of Dex between the interface of the cells and ND surface. Figure 9A shows the release characteristics of fluorescent Dex from 20 layers of the PLL−ND films, displaying a sustained release behavior. The time scale of the release properties (on the order of hours) aligned with the common time scales utilized for the incubation of Dex with the macrophages, to result in the potent knock-down of the aforementioned inflammatory cytokines. The release effect and time scale of elution were similar to those observed with the single PLL−ND layer. Coupled with the RT-PCR as well as preceding MTT and DNA fragmentation assays, it was demonstrated that the material-mediated suppression of inflammatory gene expression was due to the release of the Dex therapeutic.

MTT assays were conducted utilizing doxorubicin hydrochloride (Dox), a potent inducer of cellular apoptosis and chemotherapeutic, to serve as a counterpoint and reference toward ND-induced apoptosis/cytotoxicity levels. Whereas Dox was capable of rapidly inducing cell death, which was clearly visible *via* conventional bright-field microscopy as well as very apparent decreases in cellular viability (Figure 10A), comparisons of cell viability between cultures grown in Petri dishes/media and in the presence of NDs showed a negligible difference, further serving as an indicator that the cells were capable of remaining viable and proliferating in ND cultures. Furthermore, this observation served as further confirmation that inflammatory attenuation was Dex-induced and not due to ND-induced cell death.

The presence of NDs also did not lead to the characteristic DNA fragmentation ladder associated with apoptosis (Figure 10B). However, the addition of doxorubicin alone induced this DNA fragmentation, which served as a reference and indicator of cell death. Thus, apoptosis was not induced by the addition of NDs to the RAW 264.7 macrophage cells.

Cellular inflammation was chosen as a factor of biocompatibility for a number of reasons, including the fact that inflammation is a major process in the body that confers resistance to infection and serves as a protective barrier by generating a response for the protection from foreign bodies.[28] The translational potential of novel nanomaterials being developed for medical applications is in a large way determined by the ability of the material alone to engage in a favorable interface with surrounding biological tissue to preclude adverse secondary injury that would innately counteract any perceived benefits of the initial delivery of a therapeutic material. Such favorable interfaces include the absence of basal inflammatory cellular responses and protection against toxicity (*e.g.*, necrosis) and apoptosis (*e.g.*, programmed cell death) as well as other unfavorable biological reactions induced by the foreign material. For example, tissue-specific responses to increased expression of some inflammation genes can have a broad range of physiological effects. IL-6 expression is higher in hearts with advanced heart failure, suggesting that IL-6 expression might be a cause of heart failure.[29,30] High levels of TNFα can directly damage or sensitize liver tissue to damage.[31] There also appears to be a link between iNOS expression and cholangiocyte carcinogenesis, possibly through an increase in DNA damage.[32] In the specific context of potentially applying the ND nanofilms as implant coatings or as foundation structures for implant devices, the observation that its integration with macrophages does not lead to increased inflammatory cytokine may serve as a key benefit toward its application as a medical technology, as the ND biocompatibility eliminates the potential for secondary physiological disorders associated with material-induced cell stress.

Since the film consists of ND clusters with numerous interparticle voids, therapeutic elements, such as dexamethasone used in this work (Dex is a potent syn-

thetic member of the glucocorticoid class of steroid hormones acting as an anti-inflammatory and immunosuppressant), can be easily incorporated into the film. The intermolecular forces mediating adsorption of Dex to NDs are believed to be physical interactions, because there are no ionic groups or reactive functional groups in the Dex molecule in the mild assembly conditions. The physical interaction may involve $\pi-\pi$ stacking (both NDs and Dex have benzene rings) and dipole–dipole interaction. More importantly, NDs (2–8 nm) are in the form of aggregates with diameters of approximately 50 nm. There is an abundance of voids in each ND cluster as well as between the aggregates. Capillary force may also be involved in the load and release process. In this work, we have examined the application of a single-layer ND film for Dex incorporation. Continued studies are in process for clarifying the loading level and efficiency. In the free-floating ND solution, we observed a loading efficiency of over 10 wt %. The drug release was believed to be driven by a diffusion process because of the concentration difference the between film region and solution body. No film degradation was observed after drug release by intensive water washing. Because the film layers can be controllably constructed by the LBL process, the drug could have been incorporated into the inner layers, and thus the ND-mediated drug desorption process toward a controlled release process could be realized. Further film engineering work is ongoing toward optimized drug loading and release processes for potential ND film clinical translation. In Figure 8, we further show that inflammation in the macrophage cells can be effectively suppressed by the gradually released dexamethasone glucocorticoid molecules, which are capable of suppressing inflammatory gene induction. The resultant potent attenuation of LPS-mediated inflammation demonstrated highly efficient ND film-mediated drug release with preserved efficacy upon the interfaced macrophages. While many approaches in the form of polymeric/lipid-based materials have been explored as exciting technologies for drug-carrying solutions,[33–40] the protein-templated ND films serve as a potentially clinically applicable platform strategy for localized therapeutic delivery and drug functionalization that can be rapidly accomplished with specified dimensions.

Emerging technologies for implantable chemotherapeutic release devices are also being explored for targeted and controllable delivery of cytotoxic chemicals. Such efforts are aimed toward the suppression of generalized drug activity that can adversely affect healthy cells. Toward these anticancer applications, the investigation of material-induced inflammatory cytokine release is important due to the implications that have been presented with respect to cytokine-mediated cancer progression and predisposition, which would also negate implant functionality or lead to implant-based physiological disorders or hindrances to disease treatment. For example, IL-6 has been implicated in multiple signaling pathways, including those involving Jak/STAT, Ras/MAP kinase (MAPK), and PI-3 kinase (PI3-K)/Akt that govern processes including cancer signaling.[41] In the context of these pathways, IL-6 was shown to inhibit apoptosis through PI3-K activation.[42,43] Elevated IL-6 levels have also been shown to enhance angiogenesis and proliferation in cervical tumor cells.[44] IL-6 has also been shown to confer cellular resistance toward the chemotherapeutic agents cis-diamminedichloroplatinum and etoposide.[45] TNFα has been shown to play a significant role in inflammation-driven cancer development, which in turn supports the viability/inhibits apoptosis of precancerous and transformed cells, and the correlation between iNOS and COX-2 has also been shown to increase microvessel density/angiogenic behavior in hepatocellular carcinomas.[46–48] Therefore, in addition to the conventional application of the ND nanofilms as inflammation-suppressing coatings on implants, the NDs may also serve as a foundational technology for chemotherapeutic applications. The efficient attenuation of cytokine re-

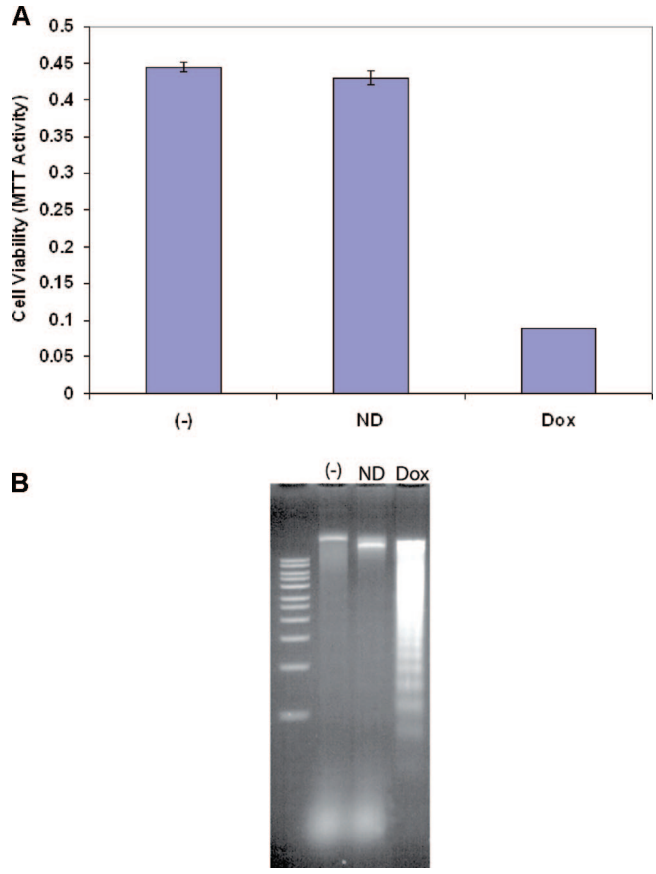

Figure 10. (A) Cell viability assay. Murine macrophage cells (RAW 264.7, ATCC) were grown in the absence (−) or presence of 25 μg/mL nanodiamonds (ND) or 2.5 μg/mL doxorubicin (Dox) for 24 h and were subjected to an MTT-based cell viability assay (Sigma-Aldrich). (B) DNA fragmentation assay. Murine macrophage cells (RAW 264.7, ATCC) were grown in the absence (−) or presence of 25 μg/mL nanodiamonds (ND) or 2.5 μg/mL doxorubicin (Dox) for 24 h and were harvested. DNA was purified and loaded on an agarose gel for analysis.

lease actively *via* ND-mediated dexamethasone elution, as well as the absence of basal cytokine secretion following cellular interaction with the NDs, demonstrates significant implications of ND-based nanofilms as interfacial materials for the inhibition of malignant tumor growth for cancer applications, given the potent impact that cytokine secretion possesses upon a multitude of cancer-relevant signaling pathways.

CONCLUSIONS

In summary, nanodiamond-based thin films were formed by using a protein-mediated LBL deposition procedure for the first time. Nanodiamonds used for the film formation were characterized by various analytical techniques, including TEM, FTIR, and TGA. Additionally, both free-floating and nanofilm-assembled ND biocompatibility was evaluated at the gene expression level that confirmed the innate benefits of the ND material due to its favorable biological interaction and lack of inflammatory cytokine up-regulated release. As increases in endogenous levels of inflammatory cytokines such as IL-6 have been shown to promote tumor progression or directly silence therapeutic activity, the observation that the NDs do not elicit adverse cellular reactions, as shown through unchanged basal cytokine release levels *in vitro* for TNFα, IL-6, and iNOS, as well as MTT assays and DNA fragmentation assays which confirmed the non-apoptotic and noncytotoxic ND properties. serves as a strong indicator for the nanofilms as a potential drug vehicle platform with translational relevance. The biofunctionality and preserved drug efficacy of the ND nanofilm as an anti-inflammation drug matrix were also demonstrated by dexamethasone anti-inflammatory transfer to the interfaced RAW 264.7 murine macrophages. Cytokine expression levels were significantly reduced, indicating efficient drug elution characteristics and stable drug interfacing with the ND nanofilm multilayers. The straightforward fabrication strategies as well as biologically amenable ND processing conditions that were employed toward developing nanofilms with rapidly tailorable thicknesses open up new possibilities in tuning drug concentration and dosage control capabilities in a bio-inert material. As such, this newly developed nanofilm demonstrates enormous potential toward biomedical applications such as serving as effective implant coatings or stand-alone drug elution technologies.

MATERIALS AND METHODS

Nanodiamond Preparation/Characterization. Nanodiamond powder was generously supplied by NanoCarbon Research Institute Ltd. and was synthesized according to previously reported detonation techniques.[13] Multiple or combinatorial methods of impurity removal were employed that include both mechanically and chemically based methodologies, as these address the removal of the spectrum of impurities (*e.g.*, non-diamond carbon, metals, *etc.*) associated with detonation ND synthesis. For example, from a mechanical context, the NDs were subjected to stirred-media milling with micrometer-sized ceramic beads, leading to disintegration of ND primary particles,[14] and chemical methodologies employed included nitric acid treatment. Thus, dispersing NDs in water could be readily achieved *via* mild sonication (Figure 1). The diameter of the primary ND particles was in the range of 2–8 nm. The NDs typically formed clusters or aggregates with a size distribution in the range of a few nanometers to hundreds of nanometers, depending on sonication conditions, the solvent used, and the settling time.

Prior to the assembly of NDs into thin films, the chemical nature and purity of the material were thoroughly investigated with various characterization techniques, including X-ray photoelectron spectroscopy (Omicron, ESCA probe) using monochromatic Al Kα radiation at a power of 300 W, Fourier transform infrared spectroscopy (FTIR, Thermal Nicolet, Nexus 870), Raman spectroscopy (Renishaw, inVia reflex microRaman, 514.5 nm laser), thermogravimetric analysis (TGA, TA Instruments, SDT 2960), and transmission electron microscopy (TEM, Hitachi H-8100).

Nanodiamond Film Fabrication. Positively charged poly-L-lysine (PLL, Sigma) backbones could be easily coated onto naturally negatively charged glass/quartz surfaces. Following the coating of the surfaces with PLL and thorough rinsing with pure water, negatively charged ND clusters were then self-assembled on top of the polymer by simply dipping the glass slide into an ND aqueous dispersion (0.1 mg/mL). The thickness of the ND thin film could be controlled by layer-by-layer assembly. ND−PLL multilayer stacking was monitored by measuring the UV–vis absorption of the film on a quartz substrate which was pretreated with concentrated NaOH to enhance the negative charge density on the quartz surface. Incorporation of drug molecules into the ND thin film was accomplished by dipping-induced adsorption followed by a drying process under steady air flow, or by coating the drugs on the NDs prior to self-assembly.

Genetic Analysis of Nanodiamond Biocompatibility and Efficacy of Biofunctionalized Nanofilms. To test the biocompatibility of the ND thin film for its potential use as a material for medical/clinical applications (*e.g.*, implant coatings), the internal cellular response effects toward incubation with both free NDs and the ND thin films in culture was investigated. For both basal inflammation and biological functionality experiments, RAW 264.7 (ATCC) cells were cultured at 37 °C in Dulbecco's modified eagle medium (DMEM) supplemented with 10% fetal bovine serum (FBS) and 5% penicillin/streptomycin. Cell growth and morphology as well as the response of genes involved in the inflammation were monitored *via* conventional microscopy (Leica Lambda DG-4, magnification × objective = 40 × 10). Specifically, interleukin-6 (IL-6), tumor necrosis factor alpha (TNFa), and inducible nitric oxide synthetase (iNOS) expression was evaluated using real-time polymerase chain reaction (RT-PCR). Innate biocompatibility studies were performed without lipopolysaccharide (LPS) stimulation to monitor cellular basal inflammation and inherent cellular response. To examine the biofunctionality of the therapeutic-activated ND thin films, dexamethasone (Dex, 1 mg/mL in ethanol), a glucocorticoid anti-inflammatory drug, was incorporated into ND clusters in the thin film (single layer, 30 min dipping). For these experiments, LPS (4 h stimulation)-mediated inflammation *in vitro* was performed to examine the suppression of inflammatory cytokine release by the Dex-incorporated ND thin film which was also examined by RT-PCR. Isolation of genetic material was accomplished by adding 1 mL of TRIzol cell lysis solution to wash the cell-coated slides. RNA isolation was done according to the manufacturer's protocol.[49] Subsequent conversion of the RNA to cDNA was performed using the I-script enzyme (Bio-Rad). Following conversion of the isolated mRNA to cDNA, RT-PCR analysis was performed (primers available upon request).

The TNFα, IL-6, and iNOS genes involved in cellular inflammation were then monitored by RT-PCR using the MyiQ Single Color

Real-Time PCR Detection System (Bio-Rad). The housekeeping gene β-actin was used to normalize levels of RNA across samples. The primer sequences used are as follows: TNFα, 5′-GGTGCCTATGTCTCAGCCTCTT-3′ and 5′-CGATCACCCCGAAGTTCAGTA-3′; IL-6, 5′-CACAGAGGATACCACTCCCAACA-3′ and 5′-TCCACGATTTCCCAGAGAACA-3′; iNOS, 5′- -3′ and 5′- -3′; β-actin, 5′-TGGAATCCTGTGGCATCCATGAAAC-3′ and 5′-TAAAACGCAGCTCAGTAACAGTCCG-3′.

Cytotoxicity Analysis of ND—Cell Interfacing. Murine RAW 264.7 macrophage cells (ATCC) were cultured in DMEM media supplemented with 10% FBS and 1% penicillin/streptomycin. To test the biocompatibility of the ND substrate, cells were grown in the presence or absence of NDs and monitored for the onset of apoptosis and/or cell death due to the presence of nanodiamonds. Doxorubicin (Dox) was used as a positive control for apoptosis and cell death. To first monitor the onset of apoptosis, a DNA fragmentation assay that visualizes the patterned degradation of DNA due to apoptosis was used. Cells were seeded at ~40% confluency with no additives or in the presence of 25 μg/mL NDs or 2.5 μg/mL Dox and grown for 24 h. DNA was collected *via* a standard harvesting protocol.[50] Briefly, cells were lysed in lysis buffer (10 mM Tris-HCl, pH 8.0, 10 mM EDTA, 1% TritonX-100) for 10 min at room temperature. Samples were collected and treated with 40 μg/mL RNase for 30 min at 37 °C and 100 μg/mL ProteinaseK for 30 min at 37 °C, followed by phenol chloroform isolation and 2-propanol precipitation. The DNA pellet was washed in 70% ethanol and resuspended in water. Samples were loaded onto a 0.8% agarose gel in sodium borate buffer, run, and stained with ethidium bromide.[51] The gel was visualized on a shortwave UV box with a CCD camera.

A second assay was also used to monitor ND biocompatibility *via* the MTT-based cell viability procedure. Again, cells seeded at ~40% confluency in media containing or lacking 25 μg/mL NDs with 2.5 μg/mL Dox used as a positive control for cell death. Cells were grown for 24 h, and the cell viability assay was performed following the manufacturer's protocol (Sigma-Aldrich) and read in a Safire multiwell plate reader (Tecan) using Magellan software (Tecan) for analysis. Samples were done in triplicate.

Acknowledgment. D.H. acknowledges support from a V Foundation for Cancer Research V Scholar Award, and the National Institute of Allergy and Infectious Diseases of the National Institutes of Health (Grant No. U54 A1065359).

REFERENCES AND NOTES

1. Niemeyer, C. M. Nanoparticles, Proteins, and Nucleic Acids: Biotechnology Meets Materials Science. *Angew. Chem., Int. Ed.* **2001**, *40*, 4128–4158.
2. Michalet, X.; Pinaud, F. F.; Bentolila, L. A.; Tsay, M.; Doose, S.; Li, J. J.; Sundaresan, G.; Wu, A. M.; Gambhir, S. S.; Weiss, S. Quantum Dots for Live Cells and in vivo Imaging, Diagnostics and Beyond. *Science* **2005**, *307*, 538–544.
3. Cui, Y.; Wei, Q. Q.; Park, H. K.; Lieber, C. M. Nanowire Nanosensors for Highly Sensitive and Selective Detection of Biological and Chemical Species. *Science* **2001**, *293*, 1289–1292.
4. Baughman, R. H.; Zakhidov, A. A.; de Heer, W. A. Carbon Nanotubes—the Route Toward Applications. *Science* **2002**, *297*, 787–792.
5. Bianco, A.; Prato, M. Can Carbon Nanotubes be Considered Useful Tools for Biological Applications. *Adv. Mater.* **2003**, *15*, 1765–1768.
6. Krüger, A. Hard and Soft: Biofunctionalized Diamond. *Angew. Chem., Int. Ed.* **2006**, *45*, 6426–6427.
7. Lacerda, L.; Bianco, A.; Prato, M.; Kostarelos, K. Carbon Nanotubes as Nanomedicines: From Toxicology to Pharmacology. *Adv. Drug Delivery Rev.* **2006**, *58*, 1460–1470.
8. Smart, S. K.; Cassady, A. I.; Lu, G. Q.; Martin, D. J. The Biocompatibility of Carbon Nanotubes. *Carbon* **2006**, *44*, 1034–1047.
9. Gruen, D. M., Shenderova, O. A., Vul, A. Y., Eds. *Synthesis, Properties and Applications of Ultrananocrystalline Diamond*; Springer: New York, 2005.
10. Hartl, A.; Schmich, E.; Garrido, J. A.; Hernando, J.; Catharino, S. C. R.; Walter, S.; Feulner, P.; Kromka, A.; Steinmuller, D.; Stutzmann, M. Protein-Modified Nanocrystalline Diamond Thin films for Biosensor Applications. *Nat. Mater.* **2004**, *3*, 736–742.
11. Yu, S. J.; Kang, M. W.; Chang, H. C.; Chen, K. M.; Yu, Y. C. Bright Fluorescent Nanodiamonds: No Photobleaching and Low Cytotoxicity. *J. Am. Chem. Soc.* **2005**, *127*, 17604–17605.
12. Fu, C. C.; Lee, H. Y.; Chen, K.; Lim, T. S.; Wu, H. Y.; Lin, P. K.; Wei, P. K.; Tsao, P. H.; Chang, H. C.; Fann, W. Characterization and Application of Single Fluorescent Nanodiamonds as Cellular Biomarkers. *Proc. Natl. Acad. Sci. U.S.A.* **2007**, *104*, 727–732.
13. Greiner, N. R.; Phillips, D. S.; Johnson, J. D.; Volk, F. Diamonds in Detonation Soot. *Nature* **1988**, *333*, 440–442.
14. Kruger, A.; Kataoka, F.; Ozawa, M.; Fujino, T.; Suzuki, Y.; Alesenskii, A. E.; Vul, A. Y.; Osawa, E. Unusually Tight Aggregation in Detonation Nanodiamond: Identification and Disintegration. *Carbon* **2005**, *43*, 1722–1730.
15. Schrand, A. M.; Huang, H. J.; Carlson, C.; Schlager, J. J.; Osawa, E.; Hussain, S. M.; Dai, L. Are Diamond Nanoparticles Cytotoxic. *J. Phys. Chem. B* **2007**, *111*, 2–7.
16. Huang, L.-C. L.; Chang, H.-C. Adsorption and Immobilization of Cytochrome c on Nanodiamonds. *Langmuir* **2004**, *20*, 5879–5884.
17. Ozawa, M.; Inaguma, M.; Takahashi, M.; Kataoka, F.; Krüger, A.; Osawa, E. Preparation and Behavior of Brownish, Clear Nanodiamond Colloids. *Adv. Mater.* **2007**, *19*, 1201–1206.
18. Liu, Y.; Khabashesku, V. N.; Halas, N. J. Fluorinated Nanodiamond as a Wet Chemistry Precursor for Diamond Coatings Covalently Bonded to Glass Surface. *J. Am. Chem. Soc.* **2005**, *127*, 3712–3713.
19. Liu, Y.; Gu, Z. N.; Margrave, J. L.; Khabashesku, V. N. Functionalization of Nanoscale Diamond Powder: Fluoro-, Alkyl-, Amino-, and Amino Acid-Nanodiamond Derivatives. *Chem. Mater.* **2004**, *16*, 3924–3930.
20. Decher, G.; Hong, J. D. Buildup of Ultrathin Multilayer Films by a Self-Assembly Process: 1. Consecutive Adsorption of Anionic and Cationic Bipolar Amphiphiles on Charged Surfaces. *Macromol. Chem. Macromol. Symp.* **1991**, *46*, 321–327.
21. Decher, G. Fuzzy Nanoassemblies—Toward Layered Polymeric Multicomposites. *Science* **1997**, *277*, 1232–1237.
22. Tang, Z. Y.; Wang, Y.; Podsiladlo, P.; Kotov, N. A. Biomedical Applications of Layer-by-Layer Assembly: From Biomimetics to Tissue Engineering. *Adv. Mater.* **2006**, *18*, 3203–3224.
23. Huang, H. J.; Marie, J.; Kajiuar, H.; Ata, M. Improved Oxidation Resistance of Single-Walled Carbon Nanotubes Produced by Arc Discharge in a Bowl-like Cathode. *Nano Lett.* **2002**, *2*, 1117–1119.
24. Pang, L. S. K.; Saxby, J. D.; Chatfield, S. P. Thermogravimetric Analysis of Carbon Nanotubes and Nanoparticles. *J. Phys. Chem.* **1993**, *97*, 6941–6942.
25. Prawer, S.; Nugent, K. W.; Jamieson, D. N.; Orwa, J. O.; Bursill, L. A.; Peng, J. L. The Raman Spectrum of Nanocrystalline Diamond. *Chem. Phys. Lett.* **2000**, *332*, 93–97.
26. Chiang, L. Y.; Upasani, R. B.; Swirczewski, J. W. Versatile Nitronium Chemistry for C60 Fullerene Functionalization. *J. Am. Chem. Soc.* **1992**, *114*, 10154–10157.
27. Raty, J. Y.; Galli, G. Ultradispersivity of Diamond at the Nanoscale. *Nat. Mater.* **2003**, *2*, 792–795.
28. Boehm, U.; Klamp, T.; Groot, M.; Howard, J. C. Cellular Responses to Interferon- Gamma. *Annu. Rev. Immun.* **1997**, *15*, 749–795.
29. Zolk, O.; Ng, L. L.; O'Brien, R. J.; Weyand, M.; Eschenhagen, T. Augmented Expression of Cardiotrophin-1 in Failing Human Hearts is Accompanied by Diminished gp130 Receptor Protein Abundance. *Circulation* **2002**, *106*, 1442–1446.
30. Corbi, P.; Rahmati, M.; Delwail, A.; Potreau, D.; Menu, P.; Wijdenes, J.; Lecron, J.-C. Circulating Soluble gp130, Soluble IL-6R, and IL-6 in Patients Undergoing Cardiac

Surgery, With or Without Extracorporeal Circulation. *Eur. J. Cardiothorac. Surg.* **2000**, *18*, 98–103.
31. Hoeflich, K. P.; Luo, J.; Rubie, E. A.; Tsao, M.-S.; Jin, O.; Woodgett, J. R. Requirement for Glycogen Synthase Kinase-3beta in Cell Survival and NF-kappaB Activation. *Nature* **2000**, *406*, 86–90.
32. Ishimura, N.; Bronk, S. F.; Gores, G. J. Inducible Nitric Oxide Synthase Up-regulates Notch-1 in Mouse Cholangiocytes: Implications for Carcinogenesis. *Gastroenterology* **2005**, *128*, 1354–1368.
33. Nardin, C.; Hirt, T.; Leukel, J.; Meier, W. Polymerized ABA Triblock Copolymer Vesicles. *Langmuir* **2000**, *16*, 1035–1041.
34. Discher, B. M.; Won, Y. Y.; Ege, D. S.; Lee, J. C.; Bates, F. S.; Discher, D. E.; Hammer, D. A. Polymersomes: Tough Vesicles Made from Diblock Copolymers. *Science* **1999**, *284*, 1143–1146.
35. Nardin, C.; Widmer, J.; Winterhalter, M.; Meier, W. Amphiphilic Block Copolymer Nanocontainers as Bioreactors. *Eur. Phys. J. E* **2001**, *4*, 403–410.
36. Nardin, C.; Thoeni, S.; Widmer, J.; Winterhalter, M.; Meier, W. Nanoreactors Based on (Polymerized) ABA–Triblock Copolymer Vesicles. *Chem. Commun.* **2000**, *15*, 1433–1434.
37. Discher, D. E.; Ahmed, F. Polymersomes. *Annu. Rev. Biol. Eng.* **2006**, *8*, 323–341.
38. Geng, Y.; Discher, D. E. Hydrolytic Shortening of Polycaprolactone-block-(Polyethylene Oxide) Worm Micelles. *J. Am. Chem. Soc.* **2005**, *127*, 12780–12781.
39. Ahmed, F.; Discher, D. E. Controlled Release from Polymersome Vesicles Blended with PEO-PLA or Related Hydrolysable Copolymer. *J. Controlled Release* **2004**, *96*, 37–53.
40. Discher, D. E.; Eisenberg, A. Polymer Vesicles. *Science* **2002**, *297*, 967–973.
41. Hirano, T.; Nakajima, K.; Hibi, M. Signaling Mechanisms Through gp130: A Model of the Cytokine System. *Cytokine Growth Factor Rev.* **1997**, *8*, 241–252.
42. Qiu, Y.; Robinson, D.; Pretlow, T. G.; Kung, H. J. Etk/Bmx, a Tyrosine Kinase with a Pleckstrin-Homology Domain, is an Effector of Phosphatidylinositol 3′-Kinase and is Involved in Interleukin 6-Induced Neuroendocrine Differentiation of Prostate Cancer Cells. *Proc. Natl. Acad. Sci. U.S.A.* **1998**, *95*, 3644–3649.
43. Deeble, P. D.; Murphy, D. J.; Parsons, S. J.; Cox, M. E. Interleukin-6- and Cyclic AMP-Mediated Signaling Potentiates Neuroendocrine Differentiation of LNCaP Prostate Tumor Cells. *Mol. Cell. Biol.* **2001**, *21*, 8471–8482.
44. Wei, L. H.; Kuo, M. L.; Chen, C. A.; Chou, C. H.; Lai, K. B.; Lee, C. N.; Hsieh, C. Y. Interleukin-6 Promotes Cervical Tumor Growth by VEGF-Dependent Angiogenesis via a STAT3 Pathway. *Oncogene* **2003**, *22*, 1517–1527.
45. Natarajan, K.; Singh, S.; Burke, T. R., Jr.; Grunberger, D.; Aggarwal, B. B. Caffeic Acid Phenethyl Ester is a Potent and Specific Inhibitor of Activation of Nuclear Transcription Factor NF-κB. *Proc. Natl. Acad. Sci. U.S.A.* **1996**, *93*, 9090–9095.
46. Cianchi, F.; Cortesini, C.; Bechi, P.; Fantappie, O.; Messerini, L.; Vannacci, A.; Sardi, I.; Baroni, G.; Boddi, V.; Mazzanti, R.; Masini, E. Up-Regulation of Cyclooxygenase 2 Gene Expression Correlates With Tumor Angiogenesis in Human Colorectal Cancer. *Gastroenterology* **2001**, *121*, 1339–1347.
47. Hendrickse, C. W.; Kelly, R. W.; Radley, S.; Donovan, I. A.; Keighley, B.; Neoptolemos, J. P. Lipid Peroxidation and Prostaglandins in Colorectal Cancer. *Br. J. Surg.* **1994**, *81*, 1219–1223.
48. Casibang, M.; Purdom, S.; Jakowlew, S.; Neckers, L.; Zia, F.; Ben-Av, P.; Hia, T.; You, L.; Jablons, D. M.; Moody, T. M. Prostaglandin E2 and Vasoactive Intestinal Peptide Increase Vascular Endothelial Cell Growth Factor mRNAs in Lung Cancer Cells. *Lung Cancer* **2001**, *31*, 203–212.
49. Perry, A. K.; Chow, E. K.; Goodnough, J. B. Differential Requirement for TANK- Binding Kinase-1 in Type I Interferon Responses to Toll-Like Receptor Activation and Viral Infection. *J. Exp. Med.* **2004**, *199*, 1651–1658.
50. Hassan, F.; Islam, S.; Mu, M. M.; Ito, H.; Koide, N.; Mori, I.; Yoshida, T.; Yokochi, T. Lipopolysaccharide Prevents Doxorubicin-Induced Apoptosis in RAW 264.7 Macrophage Cells by Inhibiting p53 Activation. *Mol. Cancer Res.* **2005**, *3*, 373–379.
51. Brody, J. R.; Kern, S. E. Sodium Boric Acid: A Tris-Free, Cooler Conductive Medium for DNA Electrophoresis. *Biotechniques* **2004**, *36*, 214–216.